RSC Pharmaceutics

ROYAL SOCIETY OF CHEMISTRY

COMMUNICATION

View Article Online
View Journal | View Issue

Cite this: *RSC Pharm.*, 2024, **1**, 227

Received 29th January 2024,
Accepted 26th April 2024

DOI: 10.1039/d4pm00024b

rsc.li/RSCPharma

In vitro evaluation of microneedle strength: a comparison of test configurations and experimental insights

Bilal Harieth Alrimawi,†[a,d] Jing Yi Lee, †[a] Keng Wooi Ng [b,c] and Choon Fu Goh *[a]

To ensure the safe and effective application of microneedles for drug delivery to the skin, the mechanical properties the microneedles and their ability to penetrate the skin are critical quality control parameters. While *ex vivo* and *in vivo* evaluations may be valuable to demonstrate actual skin penetration, they can be costly and difficult to accomplish consistently due to the inherent biological variability of the skin. On the other hand, *in vitro* approaches provide a facile means of characterising the intrinsic mechanical properties of the microneedles, independent of such biological variability. Thus, they can be used to predict and screen for the *in vivo* and *ex vivo* performance of new microneedle formulations. A variety of experimental configurations has been reported in the literature focusing on mechanical evaluations including compression tests and *in vitro* microneedle insertion studies using a non-biological skin simulant, Parafilm® M. However, there has been a paucity of data that address the comparability of the various experimental configurations. Here, we evaluated several methods for assessing the mechanical properties of microneedles *in vitro*, including their ability to insert into a non-biological skin simulant under a defined axial force, and share some insights into the experimental design and data interpretation.

Microneedles (MNs) are an array of micron-sized needles with a length up to 2000 μm, which are sufficient to penetrate the stratum corneum of human skin without damaging blood capillaries or nerve endings.[1] By creating micron-size pores in the skin, MN arrays offer a painless and active penetration enhancement strategy to increase skin permeability for drug delivery. This strategy allows drugs that do not meet the criteria for transdermal delivery, including a molecular weight <500 Da and a log *P* value of 1–3,[2] to be delivered successfully across the skin. Prime drug candidates that can benefit from this penetration enhancement strategy include very lipophilic drugs or macromolecules such as proteins and DNA.[3,4]

Skin penetration is a fundamental performance parameter of MN arrays. MN arrays should be able to withstand the external stress applied during their insertion into, or removal from, the skin. The mechanical strength of MN arrays is a quintessential criterion to avoid damage, including breaking and bending during application or handling that will greatly limit their clinical applications despite having a good drug dissolution and release profile. The types of materials used in MN fabrication and the MN geometry (including but not limited to the needle height, base diameter, inter-needle spacing and aspect ratio) are also crucial in determining the performance of MN arrays, to assure sufficient mechanical strength for skin insertion.[5,6] The mechanical strength of polymeric MN arrays is usually attributable to the polymer base, whose mechanical properties are often well understood. However, the addition of drugs and excipients to the polymer base can drastically alter the mechanical strength of the MN formulation. For these reasons, the *in vitro* mechanical characterisation of MN arrays is usually the first-line investigation to select formulations for downstream performance evaluations, including *ex vivo* or *in vivo* mechanical tests.

To ascertain the mechanical characteristics of MN arrays, an arsenal of mechanical tests including mathematical simulations have been established. In particular, compression (percentage reduction of MN length), axial and transverse failure forces are widely measured. These tests not only mimic the insertion of MN arrays into skin but also provide a simple yet efficient method to quantify the mechanical properties of MNs.[6–9] Using a texture analyser, MN arrays are typically driven towards a flat aluminium block whereupon a force is applied onto the MNs at the point of contact. With the aid of a microscope, the mode of MN failure (*e.g.*, fracture and bending), together with the reduction in the MN height, can

[a]*Discipline of Pharmaceutical Technology, School of Pharmaceutical Sciences, Universiti Sains Malaysia, Minden 11800, Penang, Malaysia.*
E-mail: choonfugoh@usm.my; Tel: +6046532074
[b]*School of Pharmacy, Faculty of Medical Sciences, Newcastle University, Newcastle upon Tyne, NE1 7RU, UK*
[c]*Translational and Clinical Research Institute, Faculty of Medical Sciences, Newcastle University, Newcastle upon Tyne, NE1 7RU, UK*
[d]*Michael Sayeg Faculty of Pharmacy, Aqaba University of Technology, Aqaba, Jordan*
† Co-first author with equal contribution.

be observed. In addition, force *vs.* displacement data can be obtained from the axial compression test to quantify the MN failure force.[10] These mechanical tests are pivotal to ensuring that the MN arrays can puncture the skin without failure (*e.g.* bending, buckling and fracturing).

Following these mechanical strength measurements, *ex vivo* evaluations are commonly carried out to assess the ability of the MN arrays to penetrate the skin. However, such *ex vivo* evaluations are subject to biological variability in the tissues, especially if they have been derived from different animal models, such as pigs, primates and rodents.[11] Hence, an artificial membrane, usually Parafilm® M sheet, was proposed and validated by Larrañeta, *et al.*[8] to mimic *ex vivo* skin in an *in vitro* MN insertion study. Although the penetration holes on the Parafilm® M sheet are commonly examined under a microscope, they can often be observed easily without one. Given that the thickness of the Parafilm® M sheet is known, the percentage of MNs penetrated as a function of the insertion depth can be estimated. This technique provides a fast and repeatable method to evaluate the skin insertion depth of MN arrays, which is important in MN formulation development.[8,12]

Since the introduction of these methods for MN mechanical evaluation and insertion study, there have been several experimental configurations reported in the literature[13–16] but these methodologies have not been validated against the original method by Larrañeta, *et al.*[8] This study attempts to compare and validate the *in vitro* MN mechanical evaluation and insertion study using Parafilm® M sheet in several experimental configurations. We also share some intricate details on various mechanical tests for MN characterisation, with a view to overcoming the challenges that may be encountered in the analysis, including the experimental setup and key experimental parameters.

The MN array formulation was first prepared using a double casting technique. In the first casting step, 200 mg of 10% w/v of polyvinylpyrrolidone (PVP) K90 solution was cast into the polydimethylsiloxane mould and centrifuged at 4020*g* (RCF) for 15 min at room temperature to push the viscous solution into the mould's cavities.[17] The excess PVP solution on the mould surface was scraped off and the content of the mould was allowed to dry at room temperature for 1 h. Next, a second layer was cast to form the MN baseplate. In this step, 300 mg of PVP K90 solution (40% w/v) was cast over the first layer and centrifuged at 4020*g* (RCF) for 15 min at room temperature. Next, the mould was placed in an oven at 40 °C for 24 h. Finally, the MN array was peeled off and kept in a desiccator for further use. The current mould makes 34 conical needles of 500 μm in length and 175 μm in base diameter.

The axial compression test was performed using the TA-XT® Plus texture analyser (Stable Micro Systems, Haslemere, UK).[18] The MN arrays were placed with the MNs facing up on a flat aluminium block of dimensions 9 × 10 cm and compressed against a metal cylindrical probe (diameter: 50 mm) of the texture analyser, as shown in Fig. 1A. The probe was set to move downwards at a speed of 0.5 mm s^{-1} until a fixed distance (0.5 mm for the current PVP MN) was reached. The maximum force obtained before MN failure was determined as the failure force.

Apart from whole MN array compression, single MN compression was also employed with a configuration as described above but replacing the probe with a smaller one (diameter: 2 mm). The probe was set to move downwards at a slower speed, *e.g.* 0.02 mm s^{-1} until the predetermined distance was reached, as illustrated in Fig. 1B. Some neighbouring MNs were removed for probe clearance where the MNs were too close to one another.

To evaluate the insertion capability, a Parafilm® M insertion study was performed by pressing folded Parafilm® M layers to MNs using a P/50 movable probe or *vice versa* using the same texture analyser. Eight sheets of Parafilm® M from BRAND GmbH (Wertheim, Germany) were stacked together to simulate the skin structure. Several experimental configurations were attempted as shown in Fig. 2:

I. MN (needles facing down) in contact with Parafilm® M sheets overlaying a dental wax (Fig. 2(I)) (modified from ref. 8 and 13)

II. MN (needles facing down) in contact with Parafilm® M sheets (Fig. 2(II))[19–21]

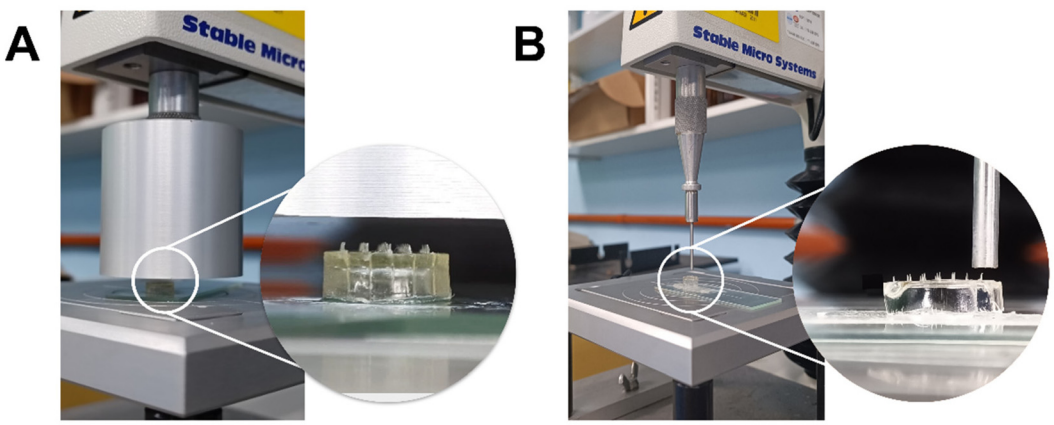

Fig. 1 Determination of MN failure force with axial compression using (A) P/50 and (B) P/2 movable metal cylindrical probe for whole MN array and single MN, respectively.

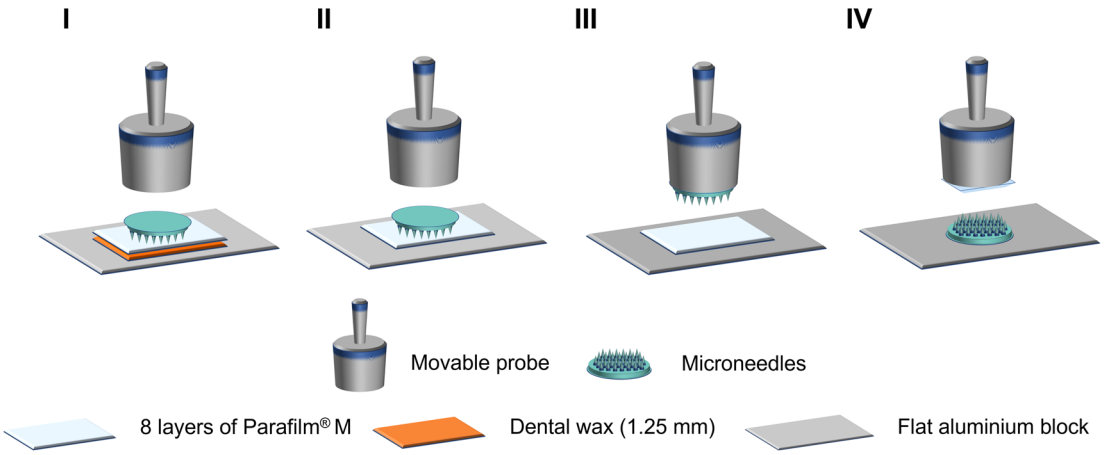

Fig. 2 Different experimental configurations for MN Parafilm® M insertion study with setup I, II, III and IV.

III. MN (needles facing down) attached to probe and Parafilm® M sheets attached to the stage (Fig. 2(III))[14–16]

IV. MN (needles facing up) attached to the stage and Parafilm® M sheets attached to the probe (Fig. 2(IV))

The probe moved downwards at 0.5 mm s^{-1} until the required force was reached (3 N was used for the current MN) and was held for 30 s. After insertion, the MN array was removed and the Parafilm® M layers were separated. The percentage of holes in each layer was determined based on eqn (1).

$$\text{Percentage of holes in Parafilm M layer}(\%) = \frac{\text{number of holes in Parafilm M layer}}{\text{total MN number}} \times 100\% \quad (1)$$

This method was also used to estimate the MN penetration depth by counting the percentage of holes created in each Parafilm® M layer. The thickness of each Parafilm® M layer was determined to be 110.0 ± 1.2 μm (n = 5; different locations of Parafilm® M sheets) using a digital micrometer (Mitutoyo®, Kawasaki, Japan). *Ex vivo* skin insertion was performed using full-thickness porcine ear skin as demonstrated by Tas, *et al.*[22] to confirm the suitability of the current MN design for skin penetration. Briefly, the MN arrays were pressed using thumb for 30 s into the excised skin with the support of dental wax and cork board before staining with methylene blue. The skin insertion ratio was calculated using eqn (2). Histological examination was also performed on the skin.[23]

$$\text{Skin insertion ratio}(\%) = \frac{\text{number of blue spots on the skin}}{\text{total MN number}} \times 100\% \quad (2)$$

Statistical analysis was conducted using IBM SPSS Statistics for Windows, version 26.0 (IBM Corp., Armonk, N.Y., USA). The data were analysed using one-way analysis of variance (ANOVA) followed by Tukey's *post hoc* test and the significant level was set at $p < 0.05$.

The force–displacement curves of PVP MN arrays are depicted in Fig. 3A. Needle failure is typically identified as a sudden drop in the force. The maximum force applied immediately before the drop is considered the MN failure force. However, the results for the whole MN array compression showed a gradual increase in the axial compression force up to 14.5 ± 3.8 N (n = 3) when it reached the distance set (0.5 mm, equivalent to the nominal MN length), with no apparent peak and subsequent drop in the force to indicate the exact moment of MN failure, although the MNs were visibly deformed after the test (Fig. 3C). In this instance, a single failure force could not be assigned but it can be surmised that the failure force was below 14.5 N.

The lack of a clear failure point in Fig. 3A(i) may indicate a very gradual compression of the MNs without buckling.[18] It may also suggest that the MNs in the array did not all fail simultaneously.[7] Collectively, the MNs would have been better able to withstand the compression force being applied than any single MN would, since the force was distributed among many MNs so the pressure on each MN was reduced. This phenomenon is similar to the 'bed-of-nails' effect widely documented for skin insertion tests.[6,24] If the MNs had failed at different times, even if some did fail by sudden buckling, the failure point of any individual MN could have been masked by the collective strength of the other MNs. Even without sudden buckling, gradual MN deformation can still impair the ability of the MNs to penetrate the skin, so it is still an important consideration. It is also worth noting that others have obtained clear failure points with the whole MN array test with different MN designs and formulations,[7] so the test outcome appears to be dependent on MN design and formulation.

The validity of the test depends upon the pressure being applied directly on to the MNs. Direct probe contact with the baseplate at any point of the force–distance measurement could result in overestimation of the MN strength. This situation can arise if not all MNs in the array make contact with the probe simultaneously, thus the pressure exerted across the MN array is uneven. Thus, the correct mounting of the MN

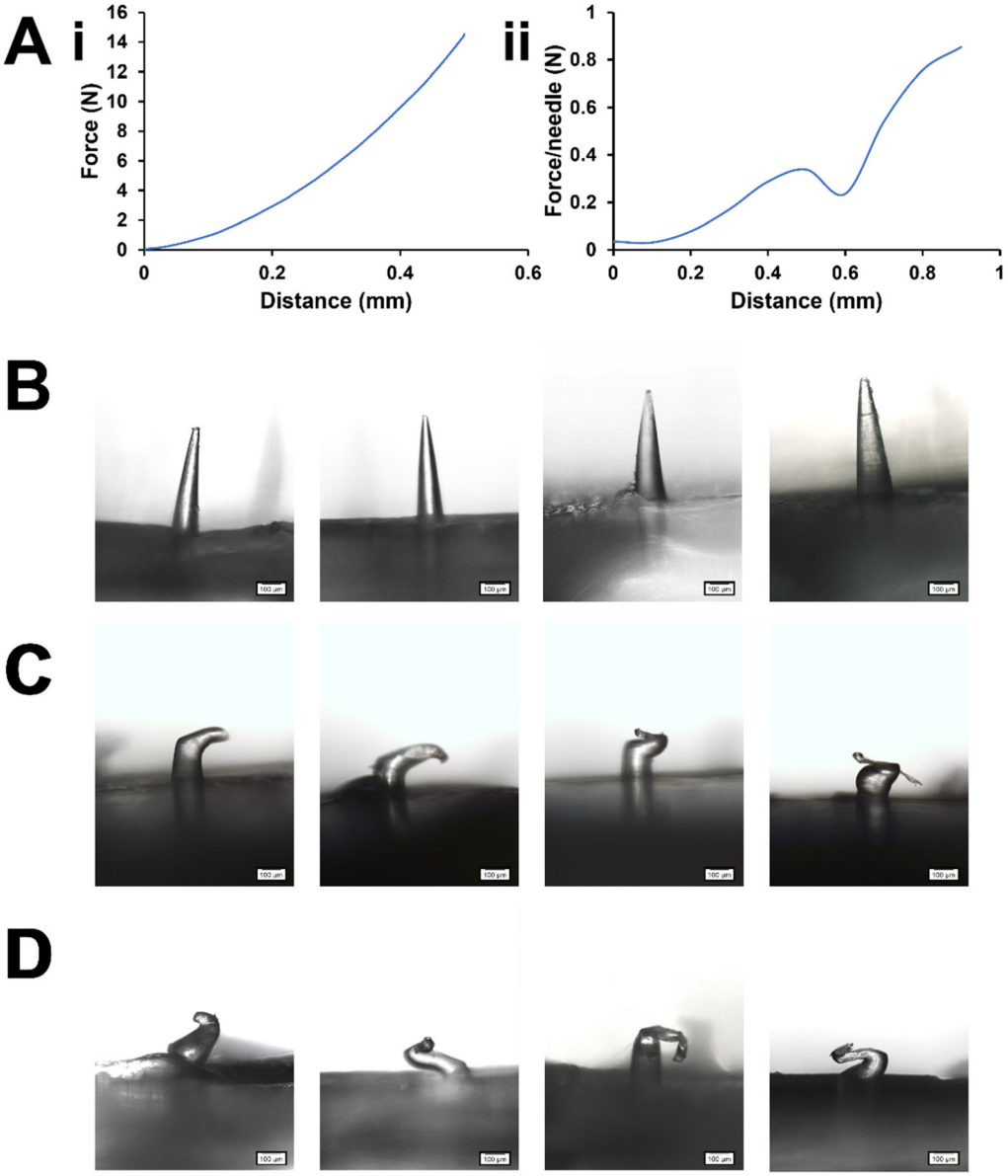

Fig. 3 (A) Force–displacement curves of PVP MN after performing axial compression test for (i) whole MN arrays and (ii) a single MN; microscopic images of PVP MN (B) before and after performing axial compression test for (C) whole MN arrays and (D) single MNs (magnification: 6.3x; scale bar: 100 μm).

array for this compression test is absolutely critical. Nevertheless, a quick check under the microscope or macro-photography could validate the mechanical changes in the MN, including MN bending or fracture (Fig. 3B–D). Alternatively, synchronous video recordings can also be used to pinpoint the compression force being exerted from the visual appearance of the MN, and *vice versa*.[25] It is also important that the baseplate is rigid and robust enough so as not to absorb any significant amount of energy from the compression by deforming, or dissipate that energy by breaking, before MN failure occurs, as this could also misrepresent the MN strength. This is an important consideration particularly if the MN and the baseplate are of different compositions, *e.g.*, where a softer material may be used for the baseplate to allow better conformity to the skin contours. This can be assured by closely monitoring the compression event visually to rule out such changes in the baseplate.

On the other hand, single MN compression gave a sudden drop in the curve at 0.32 ± 0.07 N per needle (n = 15 for a total of 3 MN arrays). It may be estimated to contribute to a total of ~11 N for the MN arrays with 34 needles. This aligns with the interpretation of the whole MN array test (whole MN array failure force <14.5 N). The mechanical changes of single MN compression can be monitored under a microscope as shown in Fig. 3D. Considering this, the single MN compression test may be preferred to verify the uncertainties in the whole MN array compression test results.

The compression test results for whole MN array and single MN may not necessarily agree with each other, but may differ somewhat for the following reasons. In the whole MN array test, the measured strength of any MN is dependent on how other MNs in the same array respond to the compression. As such, the whole MN array test may be more susceptible to variability arising from slight differences in MN length, heterogeneity in MN composition, movement of the baseplate during compression and, indeed, the compression behaviour of individual MNs in that array. The force being exerted on the whole MN array may be unevenly distributed among the MNs due to the factors above. The contact surface area may vary from MN to MN as the test progresses, and how each MN responds to that pressure may be influenced by the state of other MNs in the array at any given moment. The proposed masking effect described earlier is an example of this. Single MN tests are truly independent from each other and are not susceptible to these additional variables. Our data suggest that the single MN test can be more sensitive as it showed a clear failure point where the whole MN array test did not. However, the whole MN array test better reflects in-use scenarios for MN array patches. Both tests provide useful information about the strength of the MNs but each has its own advantages and limitations, as outlined above. At this point, it is difficult to conclude which test is more accurate or preferable. The appropriate choice of test will likely vary between studies, depending on the MN design/formulation (*e.g.* the single MN test may be challenging with densely-packed MN arrays) and the scope of the investigation. Whichever test is used, the overriding consideration is to achieve a reasonable safety factor or margin of safety to assure successful skin penetration.

The safety factor can be calculated as the ratio of the MN failure force to the skin insertion force for the MN.[26,27] The MNs should possess a safety factor >1 to achieve successful skin insertion without mechanically failing.[26] The PVP MNs had a safety factor of ~4 based on the single MN compression, suggesting that the MNs could withstand ~4 times the force needed to insert them into the skin, thus giving much assurance that the MNs would not fail mechanically during skin insertion. The interpretation of these results across different studies should take into account any differences in the polymer used, MN geometry, MN density, all of which play a major role in determining the mechanical and insertion properties of MNs. Nevertheless, a safety factor >1 is needed to guarantee skin insertion.

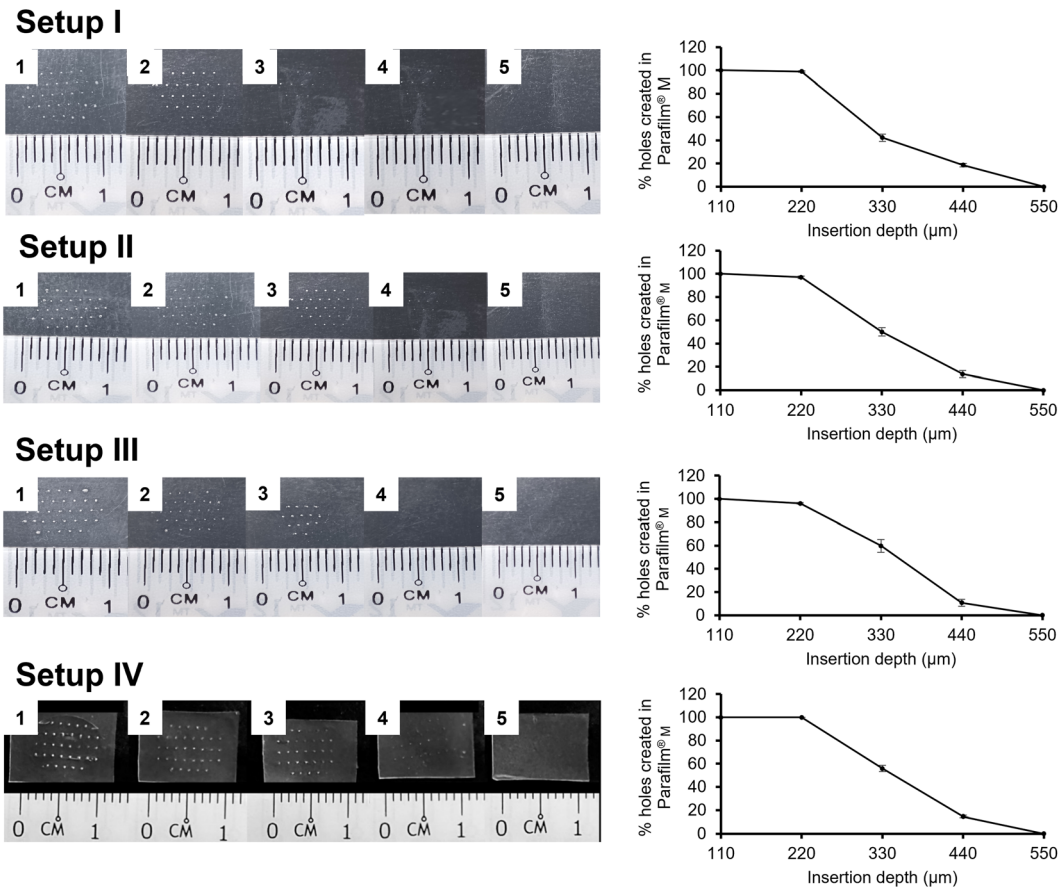

Fig. 4 Digital images of the holes created in each Parafilm® M layer after the application of PVP MN using different experimental configurations (left panel) and the corresponding profile for the percentage of holes created in Parafilm® M layers (right panel) (mean ± SD, n = 3).

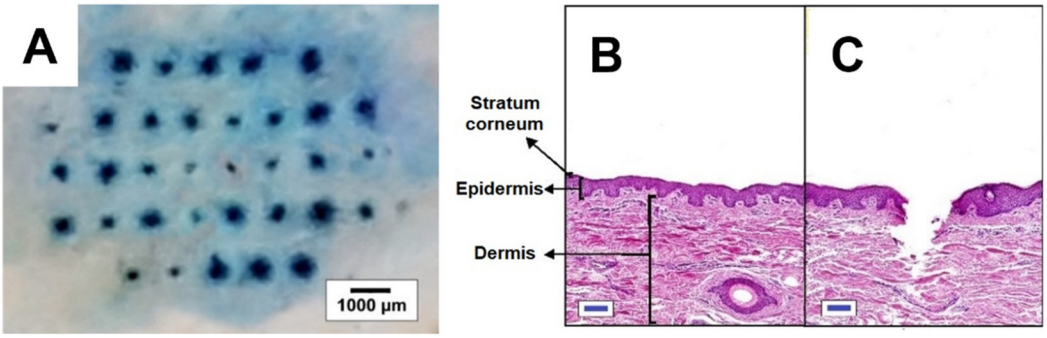

Fig. 5 (A) Digital image of PVP MN insertion into porcine ear skin and cross-sectioned view of (B) untreated skin and (C) skin pierced by MN (stained with haematoxylin and eosin; scale: 100 μm).

For *in vitro* MN insertion study, the number of holes created in each Parafilm® M layer corresponded to the number of MNs that successfully penetrated that layer (Fig. 4). Setup I was adapted from Chen, *et al.*[13] and Larrañeta, *et al.*,[8] the latter having pioneered the validation of Parafilm® M insertion test for MN mechanical evaluation and serves as the reference method. Generally, it is expected that the MNs will not insert fully into the Parafilm® M, so the penetration depth will be less than the MN length. For example, Larrañeta, *et al.*[8] reported insertion depths of ~60%. In the current study, all four setups showed successful MN insertion down to the fourth Parafilm® M layer (equivalent to ~440 μm), although the number of MNs that penetrated declined progressively down the layers (Fig. 4). This insertion depth was nearly 90% of the MN length and greater than that reported by Larrañeta, *et al.*[8] This difference was likely due to differences in the MN array design, such as the aspect ratio and pitch (centre-to-centre distance) of the MNs between these studies. Also, in the current study, there was no significant difference in the number of MN inserted at all insertion depths among the different setups ($p > 0.05$, ANOVA). Nevertheless, the literature commonly reports that MN arrays of similar strengths that penetrated up to 2–3 layers of Parafilm® M also demonstrated successful *ex vivo* and *in vivo* animal skin penetration.[12,14,28] To verify this, the PVP MN arrays used in this study have been demonstrated to achieve 93 ± 7% of skin insertion ratio *ex vivo* ($n = 20$), showing a penetration depth of 255 ± 60 μm ($n = 30$; 10 data for 3 MN arrays) as illustrated in Fig. 5. This strongly affirmed the suitability of the MN design for the validation of the *in vitro* mechanical test discussed above. A lower *ex vivo* skin penetration depth was expected as compared to the entire MN length due to the histological processing of the skin tissue.

In conclusion, the mechanical properties of MN arrays are of utmost importance to warrant the effective application of the MN formulation for drug delivery to the skin. This work has demonstrated some *in vitro* methods for evaluating the mechanical properties of MN arrays, and highlighted some important considerations when designing and executing them. A single failure force may not be assignable for the axial compression test using whole MN arrays. Alternatively, the single MN test may be more useful for single failure force determination, especially for fundamental understanding of formulation and MN design factors. For the *in vitro* MN insertion study, the different experimental configurations produced comparable results. The adoption of the test configuration is likely to depend on the experimental and MN designs. Regardless of the method, these facile tests can speed up the process of MN formulation design.

Author contributions

Bilal Harieth Alrimawi: conceptualisation, methodology, software, visualisation, investigation, validation writing – original draft preparation. Jing Yi Lee: conceptualisation, validity tests, data curation, methodology, software, visualisation, investigation, writing – original draft preparation. Keng Wooi Ng: supervision, methodology, validation, writing – reviewing and editing. Choon Fu Goh: conceptualisation, supervision, validation, project administration, funding acquisition, resources, writing – reviewing and editing.

Consent for publication

All authors have approved the content of this manuscript and have given full consent to submit this manuscript for publication.

Conflicts of interest

The authors declare no competing interests.

References

1 R. F. Donnelly, T. R. R. Singh, D. I. J. Morrow and A. D. Woolfson, In *Microneedle–mediated transdermal and intradermal drug delivery*, eds R. F. Donnelly, T. R. R. Singh, D. I. J. Morrow and A. D. Woolfson, Microneedles: Design, Microfabrication and Optimization, 2012, pp. 20–56.

2 A. Z. Alkilani, M. T. McCrudden and R. F. Donnelly, Transdermal drug delivery: Innovative pharmaceutical developments based on disruption of the barrier properties of the stratum corneum, *Pharmaceutics*, 2015, **7**, 438–470.
3 R. Jamaledin, C. Di Natale, V. Onesto, Z. B. Taraghdari, E. N. Zare, P. Makvandi, R. Vecchione and P. A. Netti, Progress in microneedle-mediated protein delivery, *J. Clin. Med.*, 2020, **9**, 542.
4 M. Kirkby, A. R. J. Hutton and R. F. Donnelly, Microneedle mediated transdermal delivery of protein, peptide and antibody based therapeutics: Current status and future considerations, *Pharm. Res.*, 2020, **37**, 117.
5 F. K. Aldawood, A. Andar and S. Desai, A comprehensive review of microneedles: Types, materials, processes, characterisations and applications, *Polymers*, 2021, **13**, 2815.
6 P. Makvandi, M. Kirkby, A. R. J. Hutton, M. Shabani, C. K. Y. Yiu, Z. Baghbantaraghdari, R. Jamaledin, M. Carlotti, B. Mazzolai, V. Mattoli and R. F. Donnelly, Engineering microneedle patches for improved penetration: Analysis, skin models and factors affecting needle insertion, *Nano-Micro Lett.*, 2021, **13**, 93.
7 J. W. Lee, J. H. Park and M. R. Prausnitz, Dissolving microneedles for transdermal drug delivery, *Biomaterials*, 2008, **29**, 2113–2124.
8 E. Larrañeta, J. Moore, E. M. Vicente-Pérez, P. González-Vázquez, R. Lutton, A. D. Woolfson and R. F. Donnelly, A proposed model membrane and test method for microneedle insertion studies, *Int. J. Pharm.*, 2014, **472**, 65–73.
9 E. Skaria, B. A. Patel, M. S. Flint and K. W. Ng, Poly(lactic acid)/Carbon Nanotube Composite Microneedle Arrays for Dermal Biosensing, *Anal. Chem.*, 2019, **91**, 4436–4443.
10 S. P. Davis, B. J. Landis, Z. H. Adams, M. G. Allen and M. R. Prausnitz, Insertion of microneedles into skin: Measurement and prediction of insertion force and needle fracture force, *J. Biomech.*, 2004, **37**, 1155–1163.
11 E. Larrañeta, R. E. M. Lutton, A. D. Woolfson and R. F. Donnelly, Microneedle arrays as transdermal and intradermal drug delivery systems: Materials science, manufacture and commercial development, *Mater. Sci. Eng., R*, 2016, **104**, 1–32.
12 B. Pamornpathomkul, T. Ngawhirunpat, I. A. Tekko, L. Vora, H. O. McCarthy and R. F. Donnelly, Dissolving polymeric microneedle arrays for enhanced site-specific acyclovir delivery, *Eur. J. Pharm. Sci.*, 2018, **121**, 200–209.
13 Z. Chen, B. Han, L. Liao, X. Hu, Q. Hu, Y. Gao and Y. Qiu, Enhanced transdermal delivery of polydatin via a combination of inclusion complexes and dissolving microneedles for treatment of acute gout arthritis, *J. Drug Delivery Sci. Technol.*, 2020, **55**, 101487.
14 L. K. Vora, P. R. Vavia, E. Larrañeta, S. E. J. Bell and R. F. Donnelly, Novel nanosuspension-based dissolving microneedle arrays for transdermal delivery of a hydrophobic drug, *J. Interdiscip. Nanomed.*, 2018, **3**, 89–101.
15 M. S. Lhernould, M. Deleers and A. Delchambre, Hollow polymer microneedles array resistance and insertion tests, *Int. J. Pharm.*, 2015, **480**, 152–157.
16 S. Demartis, Q. K. Anjani, F. Volpe-Zanutto, A. J. Paredes, S. A. Jahan, L. K. Vora, R. F. Donnelly and E. Gavini, Trilayer dissolving polymeric microneedle array loading Rose Bengal transfersomes as a novel adjuvant in early-stage cutaneous melanoma management, *Int. J. Pharm.*, 2022, **627**, 122217.
17 M. H. Ling and M. C. Chen, Dissolving polymer microneedle patches for rapid and efficient transdermal delivery of insulin to diabetic rats, *Acta Biomater.*, 2013, **9**, 8952–8961.
18 D. F. Fonseca, P. C. Costa, I. F. Almeida, P. Dias-Pereira, I. Correia-Sá, V. Bastos, H. Oliveira, M. Duarte-Araújo, M. Morato and C. Vilela, Pullulan microneedle patches for the efficient transdermal administration of insulin envisioning diabetes treatment, *Carbohydr. Polym.*, 2020, **241**, 116314.
19 H. Dawud and A. Abu Ammar, Rapidly Dissolving Microneedles for the Delivery of Steroid-Loaded Nanoparticles Intended for the Treatment of Inflammatory Skin Diseases, *Pharmaceutics*, 2023, **15**, 526.
20 U. Nagra, K. Barkat, M. Ashraf and M. Shabbir, Feasibility of Enhancing Skin Permeability of Acyclovir through Sterile Topical Lyophilized Wafer on Self-Dissolving Microneedle-Treated Skin, *Dose-Response*, 2022, **20**, 1–21.
21 M. S. Chellathurai, V. W. T. Ling and V. K. Palanirajan, Fabrication and Evaluation of Transdermal Microneedles for a Recombinant Human Keratinocyte Growth Factor, *Turk. J. Pharm. Sci.*, 2021, **18**, 96–103.
22 C. Tas, J. C. Joyce, H. X. Nguyen, P. Eangoor, J. S. Knaack, A. K. Banga and M. R. Prausnitz, Dihydroergotamine mesylate-loaded dissolving microneedle patch made of polyvinylpyrrolidone for management of acute migraine therapy, *J. Controlled Release*, 2017, **268**, 159–165.
23 S. Kim, M. S. Lee, H. S. Yang and J. H. Jung, Enhanced extraction of skin interstitial fluid using a 3D printed device enabling tilted microneedle penetration, *Sci. Rep.*, 2021, **11**, 14018.
24 W. Shu, H. Heimark, N. Bertollo, D. J. Tobin, E. D. O'Cearbhaill and A. N. Annaidh, Insights into the mechanics of solid conical microneedle array insertion into skin using the finite element method, *Acta Biomater.*, 2021, **135**, 403–413.
25 E. Smith, W. M. Lau, T. M. Abdelghany, D. Vukajlovic, K. Novakovic and K. W. Ng, Vac-and-fill: A micromoulding technique for fabricating microneedle arrays with vacuum-activated, hands-free mould-filling, *Int. J. Pharm.*, 2024, **650**, 123706.
26 J. H. Park, M. G. Allen and M. R. Prausnitz, Biodegradable polymer microneedles: Fabrication, mechanics and transdermal drug delivery, *J. Controlled Release*, 2005, **104**, 51–66.
27 E. Forvi, M. Soncini, M. Bedoni, F. Rizzo, M. Casella, C. O'Mahony and F. Gramatica, A method to determine the margin of safety for microneedles arrays, in: Proceedings of the World Congress on Engineering, 2010, pp. 1150–1154.
28 X. Jiang and P. B. Lillehoj, Microneedle-based skin patch for blood-free rapid diagnostic testing, *Microsyst. Nanoeng.*, 2020, **6**, 96.